Soil Dynamics and Earthquake Engineering 32 (2012) 87–102

Contents lists available at SciVerse ScienceDirect

Soil Dynamics and Earthquake Engineering

journal homepage: www.elsevier.com/locate/soildyn

Rocking-isolated frame structures: Margins of safety against toppling collapse and simplified design approach

F. Gelagoti, R. Kourkoulis, I. Anastasopoulos, G. Gazetas *

School of Civil Engineering, National Technical University of Athens, Greece

ARTICLE INFO

Article history:
Received 1 April 2011
Received in revised form
25 August 2011
Accepted 28 August 2011
Available online 15 September 2011

ABSTRACT

This paper aims to explore the limitations associated with the design of *"rocking-isolated"* frame structures. According to this emerging seismic design concept, instead of over-designing the isolated footings of a frame (as entrenched in current capacity–design principles), the latter are under-designed with the intention to limit the seismic loads transmitted to the superstructure. An idealized 2-storey frame is utilized as an illustrative example, to investigate the key factors affecting foundation design. Nonlinear FE analysis is employed to study the seismic performance of the rocking-isolated frame. After investigating the margins of safety against toppling collapse, a simplified procedure is developed to estimate the minimum acceptable footing width B_{min}, without recourse to sophisticated (and time consuming) numerical analyses. It is shown that adequate margins of safety against toppling collapse may be achieved, if the toppling displacement *capacity* of the frame δ_{topl} (i.e. the maximum horizontal displacement that does not provoke toppling) is sufficiently larger than the seismic demand δ_{dem}. With respect to the *capacity*, the use of an appropriate "equivalent" *rigid-body* is suggested, and shown to yield a conservative estimate of δ_{topl}. The *demand* is estimated on the basis of the displacement spectrum, and the peak spectral displacement SD_{max} is proposed as a conservative measure of δ_{dem}. The validity and limitations of such approximation are investigated for a *rigid-block* on *rigid-base*, utilizing rigorous analytical solutions from the bibliography; and for the frame structure on nonlinear soil, by conducting comprehensive nonlinear dynamic time history analyses. In all cases examined, the simplified SD_{max} approach is shown to yield reasonably conservative estimates.

1. Introduction

Current seismic design dictates that foundation systems must respond almost elastically even under strong earthquake shaking. Such code provisions are justified on the basis of the well-established conventional wisdom related to the difficulties in the (post-seismic) inspection of buried foundations (let alone their retrofitting), and on the uncertainties involved in assigning soil properties. Thus, foundations are designed to sustain increased loads compared to those of the corresponding column, by introducing appropriate *over-strength* factors [1,23].

However, over the last years there is a growing awareness that non-linear foundation response is not necessarily detrimental and may even be unavoidable during strong seismic shaking [2–6]. Three types of non-linearity at the soil–foundation level are recognized: (i) *sliding at the soil–foundation interface* when the transmitted horizontal force exceeds the available frictional resistance, (ii) *separation and uplifting of the foundation,* when the seismic overturning moment exceeds a critical value, and (iii) substantial *foundation soil yielding* to the point of mobilization of eccentric bearing capacity mechanisms. All these may considerably modify and limit the transmitted acceleration. The need to explicitly account for the aforementioned non-linear phenomena in contemporary seismic geotechnical design has emerged from the fact that the intensity of the recorded ground motions in the last 20 years has significantly exceeded the design levels. For instance during the 1994 Northridge earthquake (M_s=6.8) the maximum recorded PGA exceeded 0.90 g; during the 1995 Kobe earthquake (M_s=7.2) maximum recorded acceleration reached 0.85 g, while the 2007 Niigata-ken Oki earthquake produced an acceleration of 1.2 g. Correspondingly large were the response spectral acceleration levels.

Under such severe seismic shaking, ensuring elastic foundation response is apparently a formidable task. In fact, it may even be totally undesirable since enormous ductility demands would be imposed on the superstructure. Alternatively, allowing "plastic hinging" to develop in the foundation–soil system could be beneficial for the superstructure by bounding the inertial forces transmitted to it (through soil yielding, foundation uplifting, or both) [7–21]. This type of behavior may particularly be desirable

* Corresponding author.
E-mail address: gazetas@ath.forthnet.gr (G. Gazetas).

0267-7261/$ - see front matter © 2011 Elsevier Ltd. All rights reserved.
doi:10.1016/j.soildyn.2011.08.008

in retrofitting (existing) structures, which have been designed according to outdated seismic codes and which would obviously be unable to resist the substantially higher seismic demands of contemporary codes.

The potential effectiveness of the mechanisms of uplifting for the foundation of frame structures has recently been investigated by Gelagoti et al. [22] for a 2-storey 1-bay frame structure (Fig. 1). Since foundation plastic "hinging" is mainly in the form of rocking and uplifting of the footing, the proposed design concept is termed *rocking isolation*. Contrary to conventional capacity design, in the rocking isolation approach the footings *dimensions* are *selected* so that their moment capacity M_{ult} is smaller than that of the corresponding column M_{RD}^{C} (in that sense the rocking-isolated footings are in the ensuing referred to as "under-designed" implying that their dimensions are lower than those of the conventionally designed). Hence, in case the earthquake demand exceeds the footing capacity, the latter is intended to uplift thus limiting the distress transmitted to the column, which subsequently responds elastically (Fig. 1a). The seismic performance of a conventionally designed structure (with $B=1.7$ m square footings) was compared to a specific rocking-isolation alternative (with smaller $B=1.4$ m footings). Through static pushover and nonlinear dynamic time-history analysis (using an ensemble of 24 strong motion records), the performance of the rocking-isolated alternative was found to be advantageous in very strong seismic shaking, well in excess of the design limits (Fig. 1b). The conventionally designed structure experienced substantial damage beyond the limit of repair in most examined scenarios, and even collapsed in 3 out of 24 of them. By contrast, the rocking-isolation solution survived all seismic excitations sustaining minor to repairable column damage, but non-negligible damage to its beams. Interestingly, (at least for the cases examined) dynamic settlement was shown not to be an issue, provided that the static safety factor of the under-designed footing under its vertical load were adequately large: $FS_v > 4$.

However promising the rocking isolation concept may appear, its applicability potential is hinging on a number of critical issues. For a given frame structure, the decrease of foundation width B, and thus subsequently the reduction of the foundation moment capacity (M_{ult}), is expected to result in more effective rocking isolation. But, unfortunately, this will be directly associated with a decrease of the static safety factor FS_v, thus amplifying the risk of augmented foundation rotation, which may lead to toppling collapse, or of excessive soil yielding and intolerable settlements.

To this end, this paper investigates the margins of safety against toppling collapse of rocking-isolated frame structures, and attempts to develop a simplified design approach to conservatively estimate the minimum acceptable footing dimension.

2. Problem statement and analysis methodology

The example structure utilized in this study has been presented by Gelagoti et al. [22] and refers to an idealized 5 m wide and 7 m high 2-storey reinforced concrete (RC) frame (Fig. 2a) founded on a stiff (over-consolidated) clay stratum ($S_u=150$ kPa,

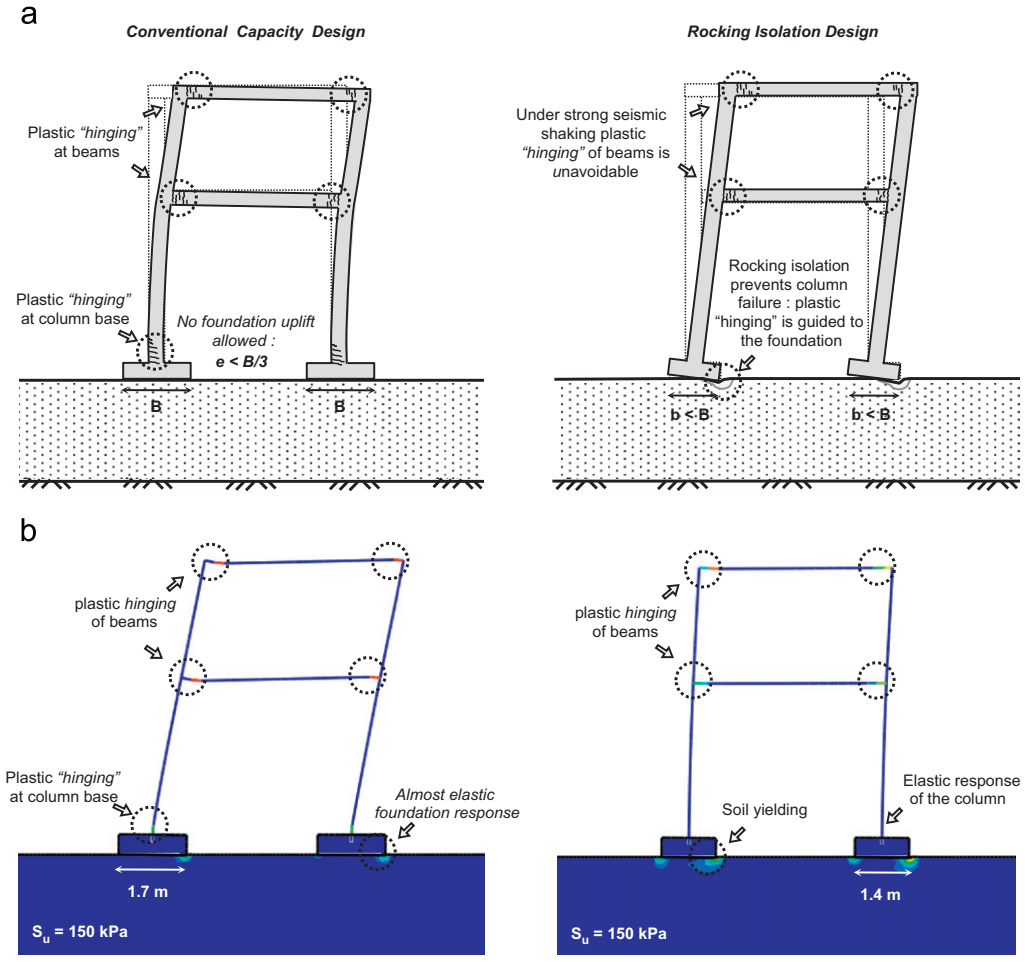

Fig. 1. Conventional Capacity Design (left column) compared with Rocking-Isolation Design (right column): (a) schematic representation of the mechanisms governing the two design alternatives, and (b) plastic strain contours of the deformed model subjected to extremely severe seismic shaking (Takatori record, Kobe 1995).

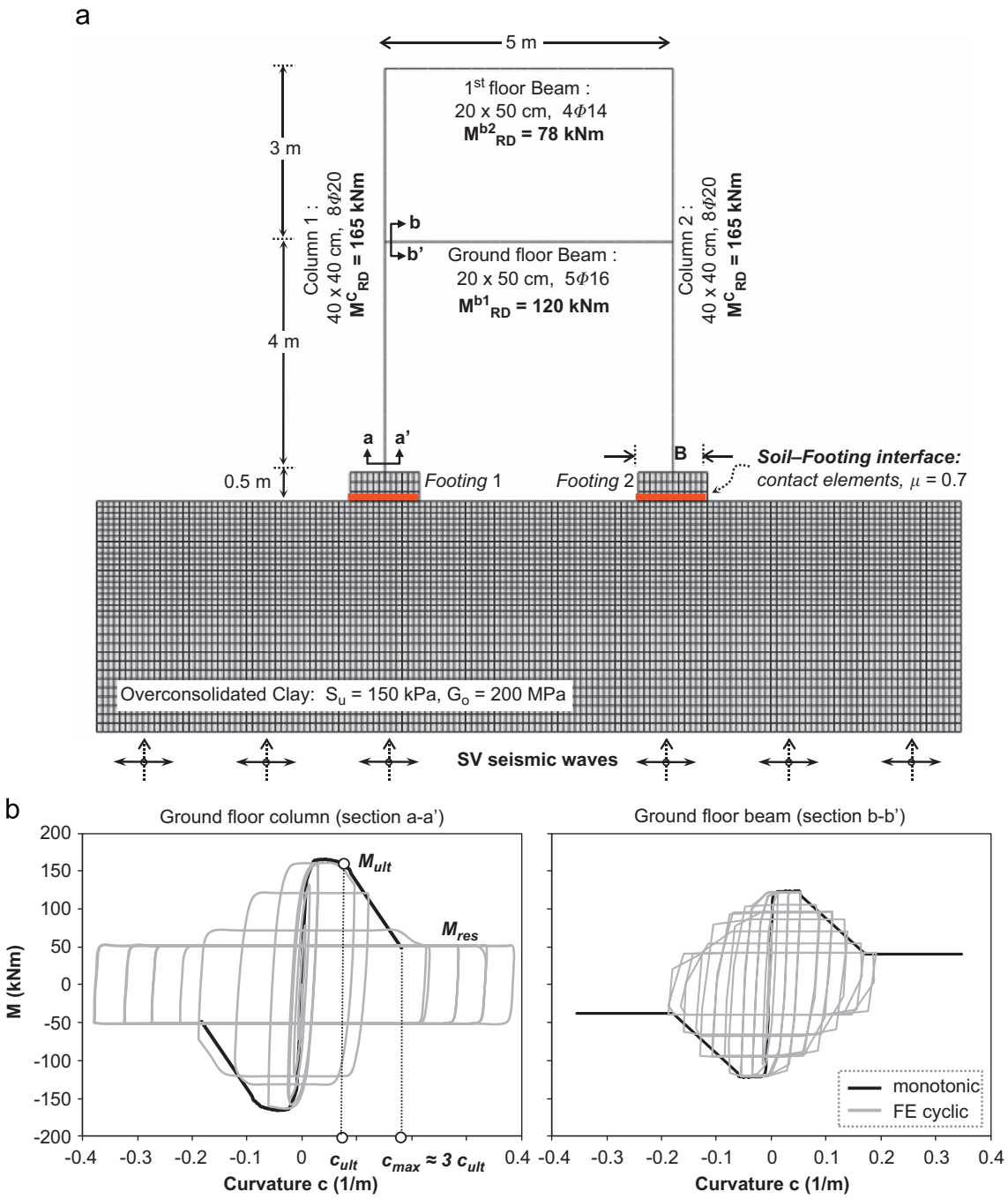

Fig. 2. (a) Geometry, member properties, and outline of the finite element (FE) model: a typical "slice" of the frame is analyzed in plane–strain, taking account of material (soil and superstructure) and geometric (uplifting and P–Δ effects) nonlinearities; (b) FE model response under dynamic loading for ground floor columns (left) and beam (right).

G_o=200 MPa). The superstructure was designed using commercial structural analysis software, in accordance with [23] and the Greek Seismic code [24], for effective design acceleration A_d=0.36 g and behavior factor q=3.5.

To meet the conventional design requirements, the foundation minimum width must be B=1.7 m. If the footing dimension is reduced (following the rocking isolation approach) the latter will respond to strong seismic shaking either through detachment from the supporting soil or soil yielding. Gelagoti et al. [22] demonstrated that foundation uplifting may be promoted against excessive soil yielding by ensuring an adequately high safety factor against vertical loads ($FS_v > 4$), which for the stiff soil conditions of the example problem may be accomplished even for the extreme case of B=1.1 m (neglecting of course the eccentricity $e < B/3$ conventional requirement).

2.1. Numerical modeling

The problem is analyzed through the finite element (FE) method. Assuming plane–strain conditions, a representative equivalent "slice" of the soil–structure system is modeled, with due consideration to material (soil and superstructure) and geometric (*uplifting* and $P-\Delta$ *effects*) nonlinearities. In order to achieve "equivalence" between the 2D and the square 3D problems, the Meyerhof [25] and Vesic [26] bearing capacity shape factor of 1.2 (for square foundation) was applied to the out of

plane dimension of the soil "slice", following the procedure proposed by Gelagoti et al. [22]. This procedure slightly overpredicts foundation settlement. Soil and footings are modeled with quadrilateral continuum elements. Nonlinear beam elements are used for the superstructure, which is connected to the soil through an interface that allows detachment and sliding. Appropriate boundary conditions are used at the lateral boundaries of the model to realistically reproduce the free-field soil response to upward propagating waves. The dynamic response of the system is simulated employing nonlinear dynamic time history analysis, applying the excitation time history at the base of the model.

Nonlinear soil behavior is modeled through a simple kinematic hardening model, with a Von Mises failure criterion and associated flow rule [27]. The full description of the model requires knowledge of only three parameters, i.e. the elastic Young's modulus E, the ultimate strength σ_y, and the yield stress σ_o. The evolution of the kinematic component of the yield stress (α) is described by the expression

$$\dot{\alpha} = E\frac{1}{\sigma_o}(\sigma-\alpha)\dot{\bar{\varepsilon}}^{pl} - \gamma\alpha\dot{\bar{\varepsilon}}^{pl} \quad (1)$$

where γ is a parameter determining the rate of decrease of kinematic hardening with increasing plastic deformation and σ the current stress.

The same kinematic hardening model is used, as suggested by Gerolymos et al. [28], to simulate the nonlinear moment–curvature response of superstructure reinforced concrete (RC) members. Model parameters are calibrated against moment–curvature (M–c) relations, obtained (up to the point of ultimate curvature c_{ult}) through RC cross-section analysis employing the X-tract [29] software. Reasonable hypothesis has been made for the metaplastic response of RC sections (for $c_{max} > c > c_{ult}$): the residual bending moment M_{res} is presumed equal to 30% of the bending moment capacity [30], and is considered to be attained for a curvature $c_{max}=3c_{ult}$. Typical calibration results are portrayed in Fig. 2b.

3. Rocking isolation of frames: minimum footing width requirement

The minimum footing width must guarantee the ability of the structure to safely undertake the imposed static and seismic loads, avoiding the development of excessive permanent foundation settlement and rotation. The criterion that must be met for the static loads is the obvious requirement of an adequate factor of safety $FS_v > 3$ (typically). In the case of seismic loading, the *rocking-isolation* concept neglects current code requirements, allowing the footing to uplift substantially: the latter is deliberately *under-designed*, so that $M_{ult} < M_{RD}^{C}$. Apparently, the decrease of the footing width, and hence of M_{ult}, leads to more effective rocking isolation. But, unfortunately, such effectiveness is also directly associated with a decrease of FS_v, thus leading to increased foundation rotation and risk of toppling. Hence, the criterion for seismic loads is the control of the developed foundation rotation, so that the structure is maintained operational, and of course safe against toppling collapse. An attempt to set out a procedure pertaining to the calculation of the minimum allowable footing width is offered in the ensuing.

3.1. The effect of footing width reduction

Utilizing the aforementioned FE modeling methodology, rocking-isolated frame structures (with under-designed footings) were subjected to pushover loading. The response in terms of horizontal *reaction force* P vs. displacement δ (at the center of mass) is displayed in Fig. 3a. Based on such results, Gelagoti et al. [22] identified three distinct phases that describe the response of rocking-isolated frames to monotonically imposed horizontal displacement. During the first phase, the frame reacts through flexural deformation up to the initiation of plastic hinging on the beams, when the framing action (development of a pair of opposite axial forces) slowly begins to deteriorate. With increasing displacement, foundation uplifting initiates as well (second phase). During the third phase, beam-to-column connections have been reduced to plastic hinges, and all of the imposed displacement is undertaken by footing rotation until the complete toppling collapse of the structure. Pushover analyses revealed (Fig. 3a) that the width of the footing controls the toppling displacement δ_{topl} *of the frame*: decreasing the footing dimension results in lower δ_{topl}. Apparently, as also indicated by the constant slope of the P–δ curve, during this third phase the flexural response is almost negligible, and the behavior up-to the point of incipient toppling is totally rocking-dominated. Therefore, the structure during this ultimate phase may be considered to have vanished to a hybrid system consisting of two 1-dof oscillators kinematically connected with the two hinged beams (Fig. 3b).

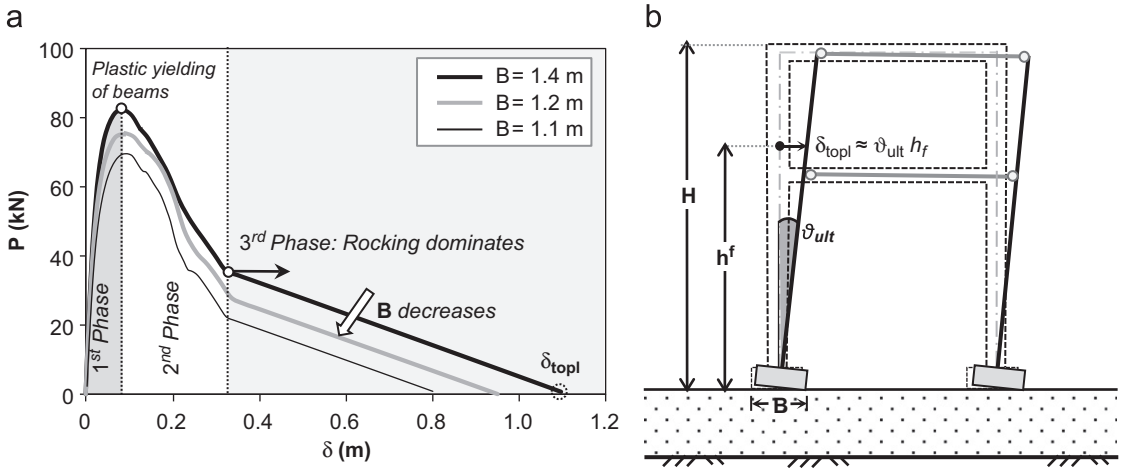

Fig. 3. (a) Static pushover P–δ response of rocking isolated frame supported on $B=1.4$ m, 1.2 m, and 1.1 m footings; (b) schematic illustration of the frame system during the ultimate phase of response, when rocking dominates: beam to column connections have vanished to hinges and the whole frame reacts to the imposed displacement through *rigid-body* rotation.

To ensure adequate margins of safety against toppling collapse, the toppling displacement of the frame δ_{topl} (i.e., the capacity) must be larger than the seismic demand δ_{dem}:

$$\delta_{dem} < \delta_{topl} \quad (2)$$

During the third rocking-dominated phase, the displacement δ at the center of mass of the structure may be easily calculated as $\delta = \theta h_f$, where h_f is the height of the center of mass and θ the footing rotation. So, apparently $\delta_{topl} = \theta_{ult} h_f$, where θ_{ult} is the frame toppling rotation. Hence, the problem of developing a simplified procedure to assess the minimum footing width to guarantee safety against earthquake-induced displacement, reduces to developing a simplified procedure to estimate δ_{dem} and δ_{topl}.

4. Simplified procedure to estimate the toppling capacity of the frame

Through the previously described FE pushover analysis of the frame–soil system, it is possible to obtain "accurately" the moment–rotation curve for the two footings (Fig. 4a), taking account of strength degradation due to second-order (P–Δ) effects, and hence estimate the frame toppling displacement capacity δ_{topl} on the basis of the minimum toppling rotation of either of its footings (the right one, in this case).

Obviously, the estimation of the exact δ_{topl} of a frame rocking on non-linear soil entails tedious numerical modeling of both the superstructure (of possibly complex geometry) and the foundation soil, taking account of both material and geometric non-linearities. This may hinder the applicability of the rocking isolation concept—hence the need for a simplified procedure is proposed, to conservatively estimate the toppling displacement capacity based solely on the geometry of the frame. To this end, the frame–soil system is gradually decomposed following a *two-step procedure*, as explained in the ensuing.

4.1. 1st step: equivalent 1-dof system response

Initially, it is attempted to reduce the frame to an appropriate 1-dof oscillator of the same footing width B and critical toppling displacement capacity δ_{topl} with the original frame structure. It is well known that the toppling rotation θ_{ult} of a 1-dof system of width B rocking on compliant inelastic soil will depend on its axial load and height. However, as demonstrated by Gelagoti et al. [22], both the actual axial load N as well as the moment to shear ratio M/Q acting on the foundation level (which determines the 1-dof system lever arm or height) constantly fluctuate, thus hindering the selection of unique values, which could be able to reproduce the original frame footing behavior.

Moreover, the moment–rotation curve of a 1-dof system (of constant lever arm and load) subjected to displacement controlled pushover loading (FE simulation), clearly manifests a qualitative disagreement with those produced for each footing during pushover of the complete frame (Fig. 4). Following these observations, the reproduction of the exact frame footing response by means of a simple 1-dof system would be apparently meaningless, and is definitely not intended at this stage. Instead, it only involves the assessment of the proper load and height of the equivalent 1-dof system that would facilitate a conservative estimate of the actual frame footing toppling rotation (i.e., that of the right footing).

To this end, Fig. 5 plots the evolution of axial load N and of the M/Q ratio (of the right footing of the frame) against the imposed lateral displacement δ, during monotonic pushover analysis the frame. Evidently, during the bending dominated first phase of the response, the axial load (Fig. 5a) on the right footing increases from its initial value $N_o = 150$ kN due to the dead load of the superstructure, to $N_{max} = 230$ kN. At the same time, i.e. before the development of plastic hinging in the beams, the ratio $M/Q \approx 2.4$ is roughly equivalent to what would be computed on the basis of conventional elastic static analysis of the frame. In the subsequent phase, as the framing action diminishes due to plastic hinging of the beams, the axial load reduces until the frame has vanished to the idealized hinged system discussed earlier, while M/Q asymptotically approaches 4.4 m, i.e. the height of the center of mass of the system. After that point, during the third phase, the axial load maintains a constant value $N \approx N_o$, whereas M/Q slightly decreases.

In view of this behavior, two idealized 1-dof systems are envisioned corresponding to the N and M/Q values acting on the right footing at the two previously identified limiting states (Fig. 5b):

(a) *Type A*, which corresponds to the ultimate stage of flexural response: a 1-dof system with mass $m = N_{max}/g \approx 2.3$ Mg, (corresponding to $N_{max} = 230$ kN) at height $h_A = 2.4$ m. Note that h_A may be readily calculated through conventional pseudo-static analysis of the structure, utilizing any commercial structural analysis software.

(b) *Type B*, which reflects the fully hinged system state during the rocking-dominated phase: a 1-dof system with mass $m = N_o/g \approx 1.5$ Mg (corresponding to $N = 150$ kN, as computed for the seismic load combination) at height $h_B = 4.4$ m.

These two "equivalent" 1-dof systems have been subjected to displacement controlled pushover loading, following exactly the same

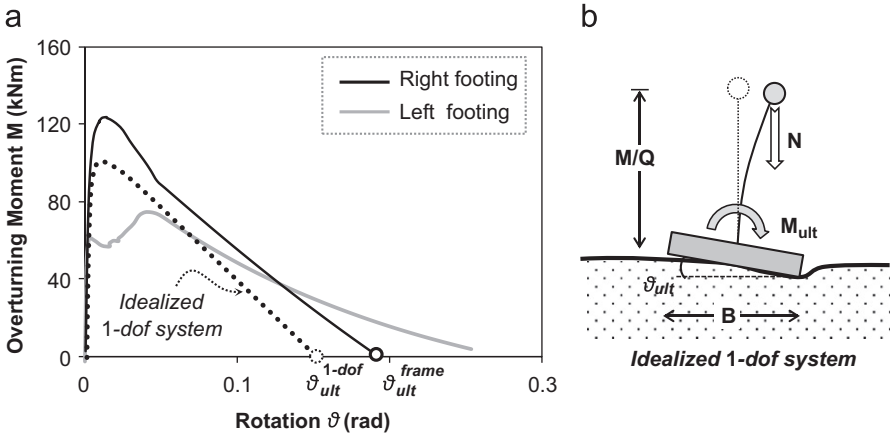

Fig. 4. Moment–rotation (M–θ) response of the two ($B = 1.4$ m) frame footings (produced through displacement-controlled pushover loading of the frame), compared with the response of idealized equivalent 1-dof system (dotted line).

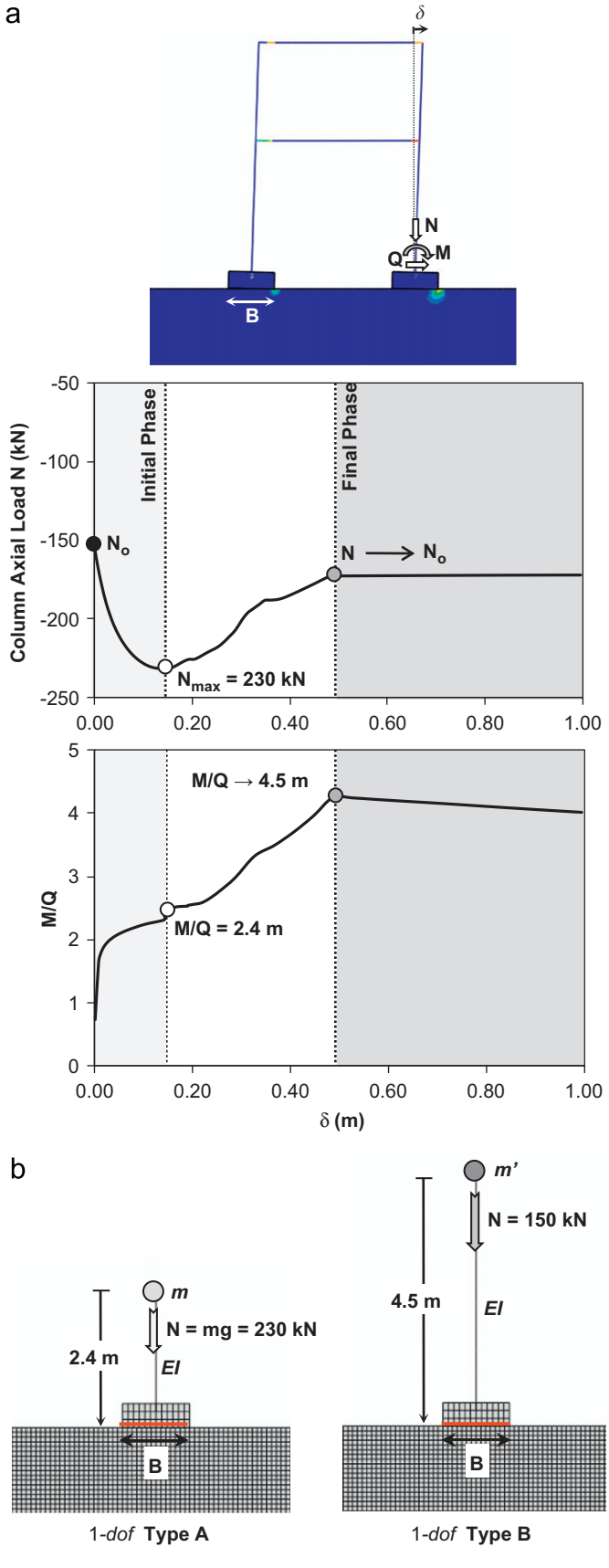

Fig. 5. Static pushover analysis of the frame (founded on $B=1.4$ m footings): (a) fluctuation of column axial load N and M/Q ratio with imposed lateral displacement δ; (b) equivalent 1-dof systems reflecting the two extreme phases of the response: Type-A corresponds to the initial phase when flexure dominates, while Type-B stems from the final (rocking dominated) phase.

analysis procedure and modeling technique as for the complete frame system; their response is compared to that of the frame in terms of moment–rotation (M–θ) response of the footing (Fig. 6). Indeed, the actual response is enveloped between the responses of the two idealized systems: while θ_{ult} is over-predicted by type A oscillator and under-predicted by type B, both approximations yield roughly the same toppling displacement capacity $\delta_{topl}\approx 58$ cm ($\theta^A_{ult}h_A=0.24$ rad $\times$ 2.4 m for type A; $\theta^B_{ult}h_B=0.13$ rad $\times$ 4.5 m for type B).

However, it should be noted that the 1-dof approximation completely ignores the residual bending moment capacity M_{res} of RC members at beam–column connections. As previously discussed, M_{res} was reasonably assumed [30] to be of the order of 30% of the corresponding bending moment capacity. This means that the plastic hinges at beam–column connections will never lose their strength completely: during the ultimate phase of response, the hinged beams will keep contributing a limited amount of restoring moment. Apparently, the 1-dof approximation assumes $M_{res}=0$, unavoidably introducing a certain degree of conservatism (which will be quantified in the sequel).

4.2. 2nd step: equivalent rigid block approach

Evidently, calculation of the toppling rotation of the equivalent 1-dof system of Step 1 still necessitates advanced soil–structure interaction analysis—an unattractive procedure for common applications. Therefore, in this step, it is attempted to further simplify the system as a rigid block of the same width, rocking on a rigid base (Fig. 7a).

To render the rigid block equivalent to the 1-dof system, its center of mass must be at a height h_o—hence the block will be twice as high as the 1-dof system. The main advantage of this approximation is that the toppling rotation of the rigid system will simply be calculated based only on its geometric characteristics as $(\theta_{ult})_{rigid}=\tan^{-1}(B/2h_o)$. The critical toppling rotation $(\theta_{ult})_{rigid}$ may be converted to critical toppling displacement $(\delta_{ult})_{rigid}$, imposed at the center of mass of the *rigid-block*, as follows:

$$(\delta_{ult})_{rigid}\approx b=B/2 \tag{3}$$

For example, for the frame founded on $B=1.4$ m footings, $(\delta_{ult})_{rigid}\approx 0.70$ m. However, according to the pushover analysis of the frame (Fig. 3), δ_{topl} is actually substantially higher, reaching 1.1 m. This difference is attributed to the previously discussed residual moment capacity M_{res} of beam plastic hinges, which is completely ignored in the rigid block approximation. For the specific case examined herein, the above conservative approximation leads

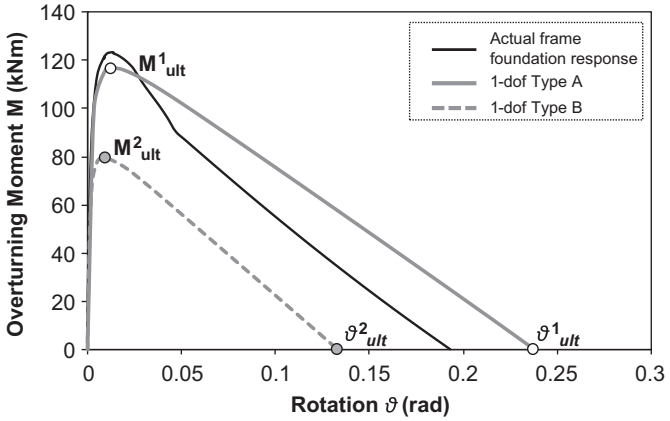

Fig. 6. Static pushover moment–rotation (M–θ) response of the right ($B=1.4$ m) footing of the frame compared with the two approximations using the two idealized 1-dof systems. At large rotations, frame response can be seen to be roughly bounded between the two equivalent 1-dof systems.

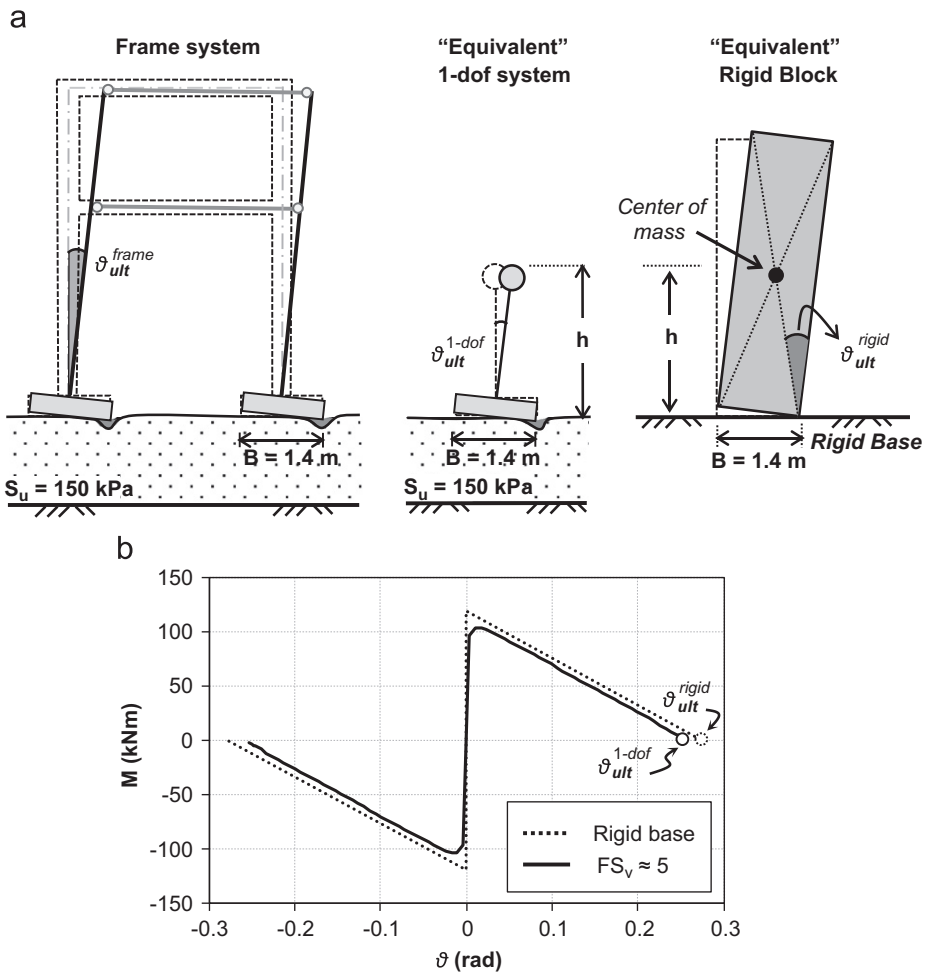

Fig. 7. (a) Problem decomposition: rocking-isolated frame on nonlinear soil (left); initial approximation of an "equivalent" idealized 1-dof system on the same nonlinear soil (middle); and further approximation to an "equivalent" rigid block rocking on rigid base. (b) Comparison of moment–rotation (M–θ) response (produced through pushover loading) of the "equivalent" idealized 1-dof system with FS_v=5 (B=1.4 m footings), with that of the rigid block on rigid base.

to under-estimation of roughly 30% of δ_{topl} (it will depend on M_{res}, and the number of participating beams).

Moreover, the rigid-block approximation inherently implies three additional fundamental assumptions:

(i) The rigid block assumption *ignores* the flexibility of the system. However, as shown earlier, during the third phase of response the effect of system flexibility is negligible since the behavior is rocking-dominated and bending is minimal.
(ii) The possible *contribution of higher modes of vibration (for m-dof structures) is ignored*. Yet, according to Bielak [31], who investigated the response of fixed base systems, the contributions of the second and higher modes to the overturning moment at the base of any classical linear system whose fundamental mode is given by a straight line vanish identically.
(iii) The rigid base assumption makes *it impossible to capture the effect of soil compliance*. Yet, the latter is expected to be negligible on the rocking response provided that the factor of safety against vertical loads is high enough—a key prerequisite of the rocking isolation concept.

To better illustrate the validity of the *rigid-base* approximation, static pushover analysis of the following systems is employed: (a) the equivalent 1-dof system with footing B=1.4 m lying on a homogenous clayey soil of undrained shear strength S_u assuming $FS_v \approx 5$, and (ii) the geometrically equivalent *rigid-block* resting on a *rigid-base*. As shown in Fig. 7b, the M–θ (moment–rotation) response of the *rigid-block on rigid-base* reasonably approximates that of the 1-dof system for large FS_v values. Naturally, the approximation is not valid for smaller safety factors, when soil yielding cannot be considered negligible. In general, and based on additional results not shown herein, the *rigid-block on rigid-base* approximation may be considered reasonable for $FS_v > 4$, which is in any case the lower allowable limit for all practical purposes.

5. Simplified approach for seismic displacement demand

As previously discussed, the estimation of the *lower acceptable* footing width requires combined knowledge of its displacement capacity δ_{topl} *and* earthquake demand δ_{dem}. Assuming that δ_{topl} can be conservatively estimated on the basis of the *rigid-block on rigid-base* approximation, the problem reduces to establishing a procedure to obtain conservatively the displacement demand δ_{dem} for a specific seismic motion. An initial rational approach towards this could be that proposed by Priestley et al. [33], who estimate δ_{dem} of a motion based on the displacement spectrum of an equivalent 1-dof oscillator, $SD(T_{eff})$.

However, in accord with the relevant bibliography (e.g. [16,32]), T_{eff} of a rocking system constantly changes during shaking, rising from zero (in the case of a rigid block "tied" to its base) to infinity once the toppling condition has been met (Fig. 8). Hence, T_{eff} cannot be known a-priori and consequently $SD(T_{eff})$ cannot be

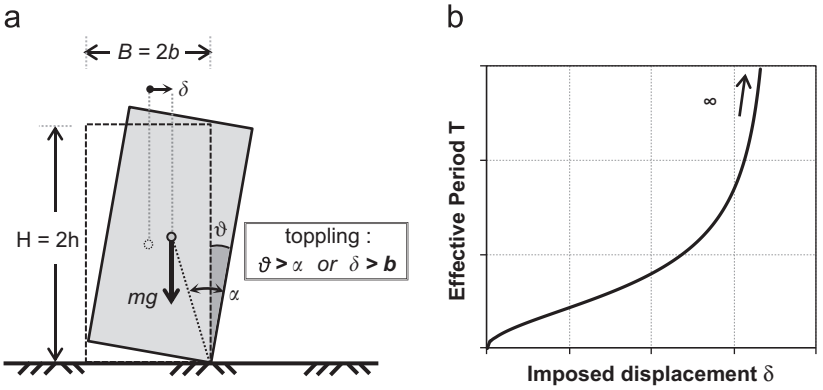

Fig. 8. Rigid block lying on a rigid base: (a) problem geometry; and (b) evolution of effective period T with displacement δ. At the state of incipient toppling, T tends to infinity.

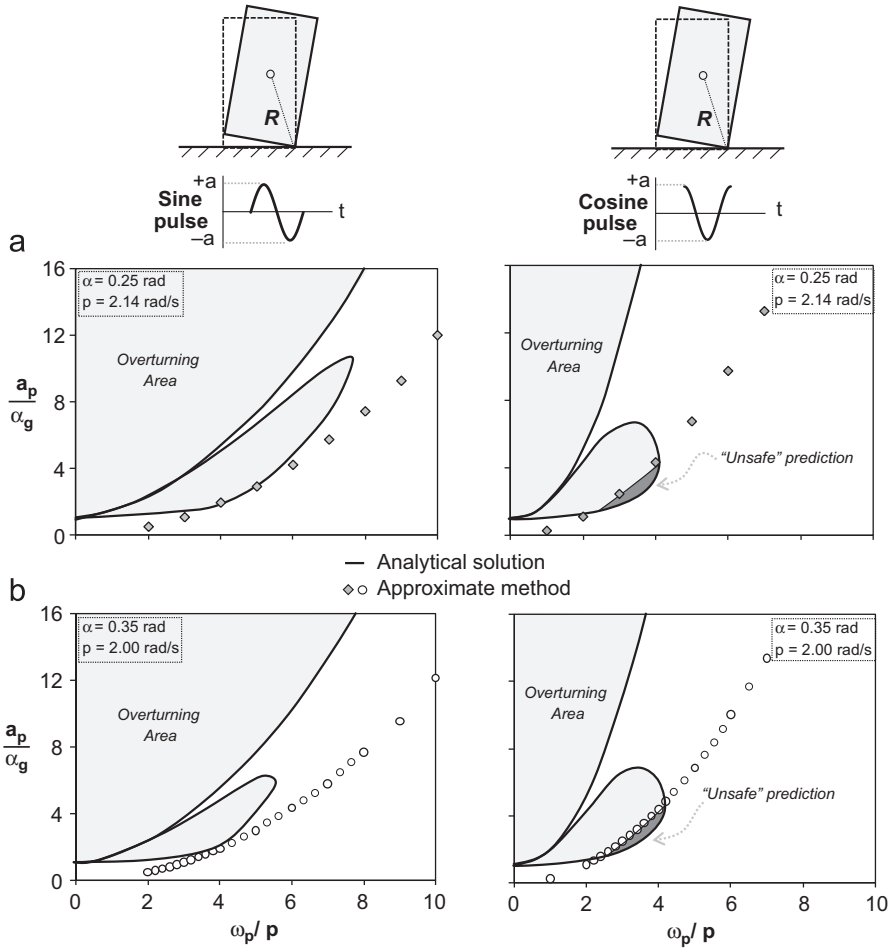

Fig. 9. Comparison of the simplified method (based on the maximum spectral displacement SD_{max}) with the rigorous analytical solution of [39] for a rigid body rocking on a rigid base, subjected to idealized base excitation: one-cycle sine pulse (left column) and one-cycle cosine pulse (right column). Non-dimensional toppling acceleration $a_p/\alpha g$ as a function of the normalized excitation frequency ω_p/p, for: (a) a smaller block of $p=2.14$ rad/s and $\alpha=0.25$ rad, and (b) a larger block of $p=2.0$ rad/s and $\alpha=0.349$ rad.

easily defined: although [33] had proposed an iterative simplified method to compute T_{eff} and estimate the rotation θ of a rocking system on the basis of *SD*, Makris and Konstantinidis [34] have shown that rocking response cannot be approximated by 1-dof oscillator-based methodologies, as the two systems are fundamentally different (stiffness, damping, and restoring mechanisms).

Taking account of the above limitations, the peak spectral displacement SD_{max} is proposed as a conservative measure of the *upper bound* displacement demand (i.e. independently of T_{eff}). Note that SD_{max} is only adopted as a conservative index of the maximum anticipated seismic displacement demand, which will not necessarily develop during seismic shaking. The validity and limitations of this simplified approximation are investigated in the following sections for two classes of problems: (i) for a *rigid-block* on a *rigid-base*, and (ii) for the frame structure on nonlinear soil. Extensive studies have been reported in the literature for the

first problem, which have resulted in rigorous analytical solutions; the investigation of the second class of problems will be made employing numerical simulations.

6. Validation of the simplified (SD_{max}) approach for a rigid block on rigid base

The issue of earthquake-induced rocking of *rigid blocks* on *rigid base* has been studied very thoroughly over the last decades [7,32,35–38], revealing the sensitive and highly nonlinear nature of the problem. Most researchers (e.g. [16,39]) conclude that the overturning (or toppling) of such structures is quite unpredictable – *if not chaotic* – even for idealized cycloidal pulses as excitation. Hence, attempting to accurately quantify the toppling potential of a seismic motion (for a given *rigid block*) utilizing the simplified SD_{max} criterion would be overly optimistic. Instead, the present study attempts to validate SD_{max} as a *conservative upper-bound* of earthquake displacement demand δ_{dem}, for which toppling will not take place, for a rigid block on rigid base subjected to: (a) cycloidal (sine and cosine) pulses, and (b) Ricker wavelets.

6.1. Rigid block subjected to sine and cosine pulses

A rigid block of width $B=2b$ and height $H=2h$ (Fig. 8) is characterized by its slenderness ratio $\alpha=\tan^{-1}(b/h)$ and the frequency parameter p

$$p=\sqrt{3g/4R} \tag{4}$$

Notice that the latter can be seen as a measure of the dynamic characteristics of the block and decreases with the size of the block. Zhang and Makris [39] investigated analytically the transient rocking response of free-standing rigid blocks subjected to trigonometric (sine and cosine pulses) base excitation. They concluded that under one-cycle cycloidal excitation the block may topple either after one impact (mode 1), or without impact (mode 2), while a surprising "safe region" exists between the two modes. These rigorous analytical results are used herein as a yardstick to ensure that the SD_{max} approach is indeed capable of producing reasonable-conservative estimates.

Two example problems are studied: a "large" block of $p=2.0$ rad/s and $\alpha=0.35$ rad, and a "small" block of $p=2.14$ rad/s and $\alpha=0.25$ rad. Both are subjected to one-cycle sine and cosine pulses of amplitude a and cyclic frequency ω_p. The acceleration amplitude required to cause overturning of the block is defined as the toppling acceleration a_p. Fig. 9 compares the simplified SD_{max} approach with the analytical solution of Zhang and Makris [39]. The non-dimensional toppling acceleration $a_p/\alpha g$ is plotted as a function of normalized excitation frequency ω_p/p for a sine (left column) and a cosine pulse (right column). The shaded areas in Fig. 9a and b depict the overturning areas of the two rigid blocks. Evidently, the non-dimensional toppling acceleration $a_p/\alpha g$ increases exponentially with ω_p/p, which means that it increases with both increasing excitation frequency *and* increasing size of the block ($1/p\propto\sqrt{R}$). The simplified approach is employed to compute the pulse acceleration amplitude $(a_p)_{SD}$ required to produce a displacement spectrum with SD_{max} equal to the toppling displacement δ_{ult} of each block: $\delta_{ult}=40$ cm for the large block ($p=2.0$ rad/s); $\delta_{ult}=63$ cm for the smaller one ($p=2.14$ rad/s). By no means should this be viewed as an attempt of capturing the detailed complex response. For the sine pulse, the simplified approach provides a conservative estimate of a_p for the whole frequency range. However, for the cosine pulse it provides a conservative estimate for

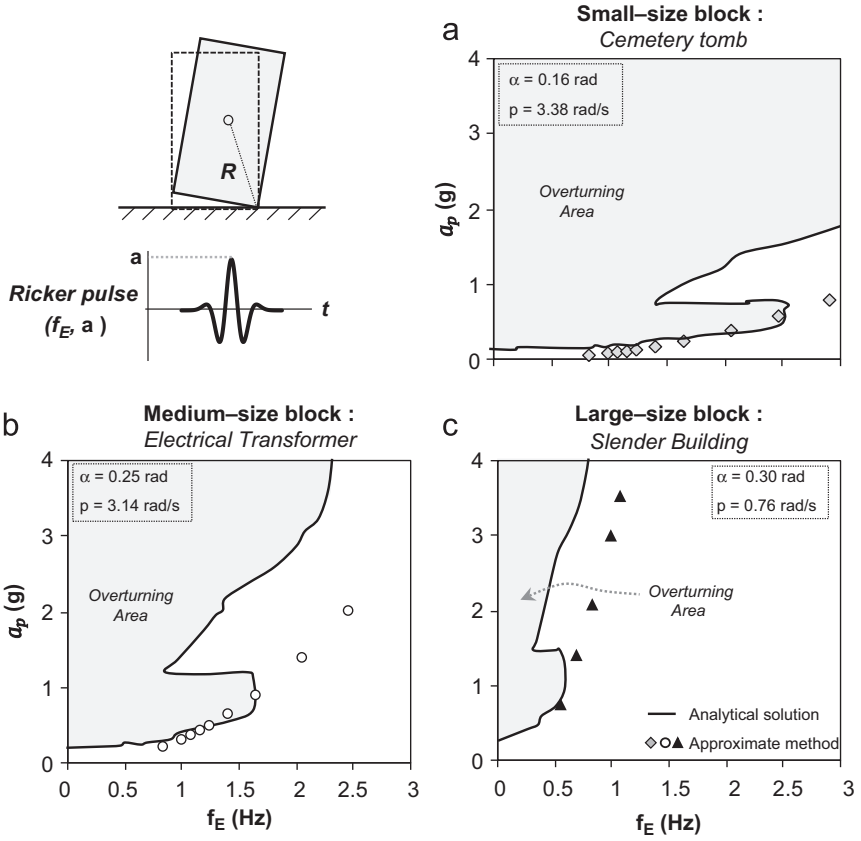

Fig. 10. Comparison of the simplified method (based on SD_{max}) with the numerical solution of Gerolymos et al. [28,38] for a rigid body rocking on a rigid base, excited by Ricker pulses. Toppling acceleration a_p as a function of excitation frequency f_E for: (a) a small-size block (tombstone) of $p=3.38$ rad/s and $\alpha=0.16$ rad, (b) a medium-size block (electrical transformer) of $p=3.14$ rad/s and $\alpha=0.25$ rad, and (c) a large-size block (slender building) of $p=0.76$ rad/s and $\alpha=0.30$ rad.

lower and higher values of the frequency ratio ($\omega_p/p \le 1.8$ and $\omega_p/p \ge 4.3$), becoming marginally *unconservative* for intermediate frequencies ($1.8 < \omega_p/p < 4.3$). But this latter "unsafe area" is of negligible practical significance for the systems under consideration: for low rise frames p ranges between $0.6 < p < 1$, and consequently the ratio ω_p/p is always greater than 4 for pulse periods $T_p < 1.6$ s (i.e., almost the complete earthquake period range).

6.2. Rigid block subjected to Ricker pulses

Although the preceding analysis has yielded encouraging results, the simplified SD_{max} approach needs to be further validated against more realistic – yet still idealized – pulses. To this end, SD_{max} predictions are compared to rigorous numerical analysis results, referring to the overturning of rigid blocks subjected to Ricker pulses. Gerolymos et al. [38], based on validated numerical analysis results, employed artificial neural networks to derive closed-form analytical expressions for predicting the overturning acceleration a_p, as a function of rigid block geometry (α and p) and excitation frequency f_E for three example problems: (i) a small-size block of $\alpha = 0.16$ rad and $p = 3.38$ rad/s, simulating a *cemetery tomb*; (ii) a medium-size block of $\alpha = 0.25$ rad and $p = 3.14$ rad/s, simulating an *electrical transformer*; and (iii) a large-size block of $\alpha = 0.30$ rad and $p = 0.76$ rad/s, simulating a *slender building*.

Fig. 10 depicts the comparison of the simplified SD_{max}-based prediction with the more rigorous solution of Gerolymos et al. [38], in terms of toppling acceleration a_p as a function of excitation frequency f_E of the Ricker pulse (the shaded areas represent the overturning regions of the three rigid blocks, according to the rigorous solution). Interestingly, for these more realistic ground motions, increasing the block size increases the conservatism of the simplified SD_{max}-based method, in accord with our previous observation.

7. Validation of the simplified approach for the 2-storey frame on inelastic soil

In the previous sections, the SD_{max} approach was validated for *rigid blocks* on a *rigid base*, subjected to idealized pulses. This section further verifies the effectiveness of the simplified approach for the actual problem: the 2-storey frame founded on nonlinear soil, subjected to Ricker pulses and real seismic records.

The analysis is conducted for the same example frame founded on $B = 1.1$ m footings (Fig. 11a): the minimum footing dimension that satisfies the criterion of $FS_v > 3$ (for static loads). Based on the M–θ response of the two frame footings (Fig. 11b), the toppling rotation is $\theta_{ult}^{frame} = 0.143$ rad, corresponding to $\delta_{topl} = 71$ cm (at the center of mass of the frame). Note that according to the rigid-block approximation $\delta_{topl} = 55$ cm (due to the previously discussed assumption of $M_{res} = 0$ at beam plastic hinges).

Therefore, according to the simplified approach any motion with $SD_{max} < \delta_{topl}$ should not provoke toppling of the frame. Hence, the validation of the simplified approach will consist of shaking the frame (at the base of the FE model) with seismic excitations (Ricker wavelets and real records), appropriately scaled (in amplitude) so that their SD_{max} is marginally lower than the toppling displacement δ_{topl} of the frame (e.g., $SD^- = 0.9\delta_{topl}$). [Note that for the considered stiff soil profile, the 1-d soil amplification is negligible].

In an attempt to further investigate the safety margins provided by the SD_{max} approach, the applied seismic excitations are subsequently also scaled to $SD_{max} = 1.1\delta_{topl}$ ($= 78$ cm), denoted hereafter SD^+.

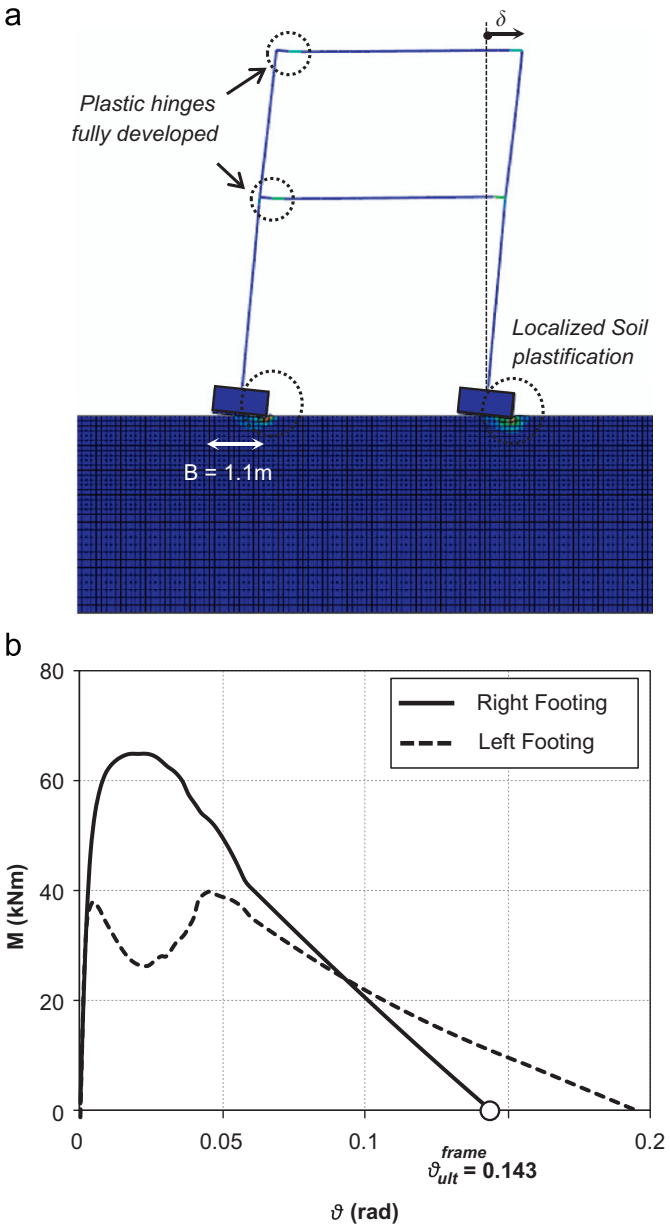

Fig. 11. Static pushover analysis of the example frame with $B = 1.1$ m footings: (a) deformed mesh with superimposed plastic strain contours, just before toppling collapse; and (b) M–θ response of the two frame footings. The moment capacity and the ultimate rotation θ_{ult} of the two frame footings are affected by the fluctuation of the axial load N and the M/Q ratio.

7.1. Ricker pulses

Ricker pulses of seven different characteristic frequencies, $f_E = 0.4$, 0.5, 0.65, 0.85, 1.0, 1.25, and 1.5 Hz, are utilized. All pulses are scaled so that their SD_{max} is equal to SD^+ or SD^- (Fig. 12a). Hence, their scaled (to yield SD_{max}) acceleration amplitude is the predicted toppling acceleration $(a_p)_{SD}$ of the system, according the simplified method.

The validity of this prediction is verified through nonlinear dynamic FE time-history analysis of the frame, subjected to the seven Ricker pulses, progressively increasing their amplitude until collapse (i.e., toppling of the frame). The minimum acceleration amplitude of each motion, which provokes (toppling) collapse constitutes the "actual" (rigorously computed) toppling acceleration a_p. Fig. 12b compares the predicted $(a_p)_{SD}$ toppling acceleration (applying the simplified SD_{max} approach) to the actual a_p

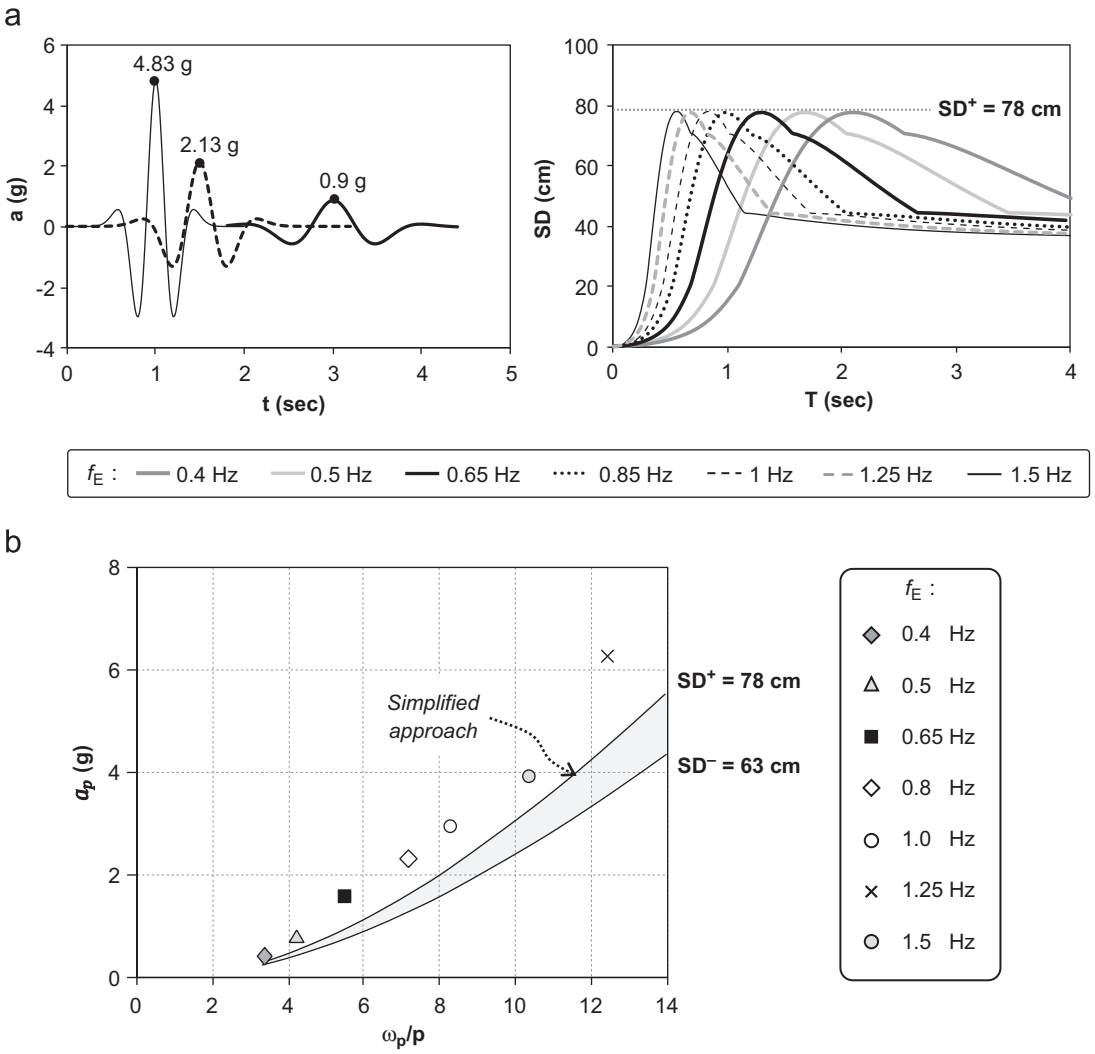

Fig. 12. Comparison of simplified approach (based on SD_{max}) with dynamic time history analysis of the frame on nonlinear soil subjected to Ricker pulses of various dominant frequencies f_E: (a) acceleration time histories and displacement response spectra SD of scaled (to produce max $SD^+=78$ cm) Ricker pulses—for clarity, only three time histories are shown, corresponding to the two extremes ($f_E=1.5$ Hz and 0.65 Hz), and an intermediate frequency pulse ($f_E=1$ Hz); (b) comparison of FE computed toppling acceleration a_p with the prediction of the simplified SD_{max} approach, as a function of non-dimensional excitation frequency ω_p/p.

(according to the results of the nonlinear dynamic FE analysis of the frame), as a function of non-dimensional excitation frequency ω_p/p. For all frequencies examined, the simplified approach yields a reasonably conservative prediction, while the margin of safety increases with increasing ω_p/p (as was the case with the *rigid-block* on *rigid-base*).

7.2. Real records

An ensemble of 18 recorded earthquake motions (from the US, Europe, and Asia) are utilized as seismic excitation. The records cover a wide range of key characteristics, enabling us to capture the effects of various parameters, such as *PGA* and *PGV*, *SA* and *SD*, frequency content, duration, number of strong motion cycles.

To apply the simplified SD_{max} approach, all records are scaled to $SD^-=63$ cm and $SD^+=78$ cm (Table 1). The scaled to $SD^+=78$ cm time histories are shown in Fig. 13. Quite interestingly, in most cases (Fig. 13a) the original records had to be substantially amplified (scaled *up*) to yield the target spectral displacements; few exceptions (in which the original records had to be scaled *down* to yield $SD^+=78$ cm) are shown in Fig. 13b. The displacement spectra SD of the scaled accelerograms are shown in Fig. 13c; in most cases, the resulting spectral accelerations SA overly exceed the design spectrum of the frame (Fig. 13d).

The validity of the prediction (applying the simplified SD_{max} approach) is verified through dynamic nonlinear time-history analysis of the frame, subjected to the aforementioned records scaled at SD^+ and SD^-. For all cases examined, toppling is avoided for the SD^- scaled records. In other words, for an SD value just 10% lower ($SD^-=0.9\delta_{ult}$) than the toppling displacement ($\delta_{ult}=71$ cm) of the $B=1.1$ m footings, the frame will not collapse (overturn).

Quite encouragingly, even for the SD^+ scaled seismic motions ($SD^+=1.1\delta_{ult}$), in most cases the frame does not topple (but experiences substantial distortion). Yet, in only 2 (and indeed highly amplified) out of the 18 records examined, the SD^+ scaled ground motion leads to toppling collapse of the frame. This can be seen as an indication of the degree of conservatism of the simplified approach in the case of real seismic excitations: even for imposed SD 10% higher than the toppling displacement δ_{ult}, toppling collapse is avoided in most cases. The toppling potential of real seismic excitations is investigated in more detail in the ensuing, attempting to derive deeper insights into the prevailing factors affecting the response.

Table 1
Scale factors applied to each record to achieve the required peak spectral displacement *SD*, and summary of analysis results (toppling or not).

Record	Earthquake	Original PGA (g)	For SD^-=63 cm			For SD^+=78 cm		
			Scale factor	Scaled PGA (g)	Toppling	Scale factor	Scaled PGA (g)	Toppling
Treasure-Island	Loma Prieta, 1989	0.08	5.47	0.44	NO	7	0.56	NO
Kalamata O.T.E	Kalamata, Greece, 1986	0.25	3.5	0.88	NO	4.48	1.12	NO
ElCentro000	ElCentro, 1940	0.31	2.35	0.73	NO	3	0.93	NO
GIC090	**San Sanvaldor, 1986**	**0.69**	**1.99**	**1.38**	**NO**	**2.55**	**1.76**	**YES**
Lucerne000	Landers, 1992	0.68	1.7	1.16	NO	2.18	1.48	NO
Izmit	Kocaeli, 1999	0.22	1.42	0.31	NO	1.82	0.4	NO
JMA000	**Kobe, 1995**	**0.82**	**1.34**	**1.09**	**NO**	**1.71**	**1.4**	**YES**
Duzce-Bolu000	Duzce, 1999	0.73	1.22	0.89	NO	1.56	1.14	NO
Erzincan-ew	Erzincan, 1992	0.49	1.09	0.53	NO	1.39	0.68	NO
Rinaldi218	Northridge, 1994	0.83	1.02	0.84	NO	1.3	1.08	NO
Sylmar Olive view-090	Northridge, 1994	0.6	1.02	0.61	NO	1.3	0.78	NO
Jensen Filtration Plant-292	Northridge, 1994	0.59	0.8	0.47	NO	1.02	0.6	NO
Pacoima Dam254	San Fernado, 1971	1.22	0.78	0.95	NO	1	1.22	NO
Takatori000	Kobe, 1995	0.61	0.53	0.32	NO	0.67	0.41	NO
Tabas-LN	Iran, 1978	0.84	0.47	0.39	NO	0.6	0.5	NO
Duzce000	Duzce, 1999	0.35	0.42	0.15	NO	0.54	0.19	NO
Lucerne275	Landers, 1992	0.7	0.38	0.27	NO	0.49	0.34	NO
Duzce270	Duzce, 1999	0.54	0.38	0.2	NO	0.48	0.26	NO

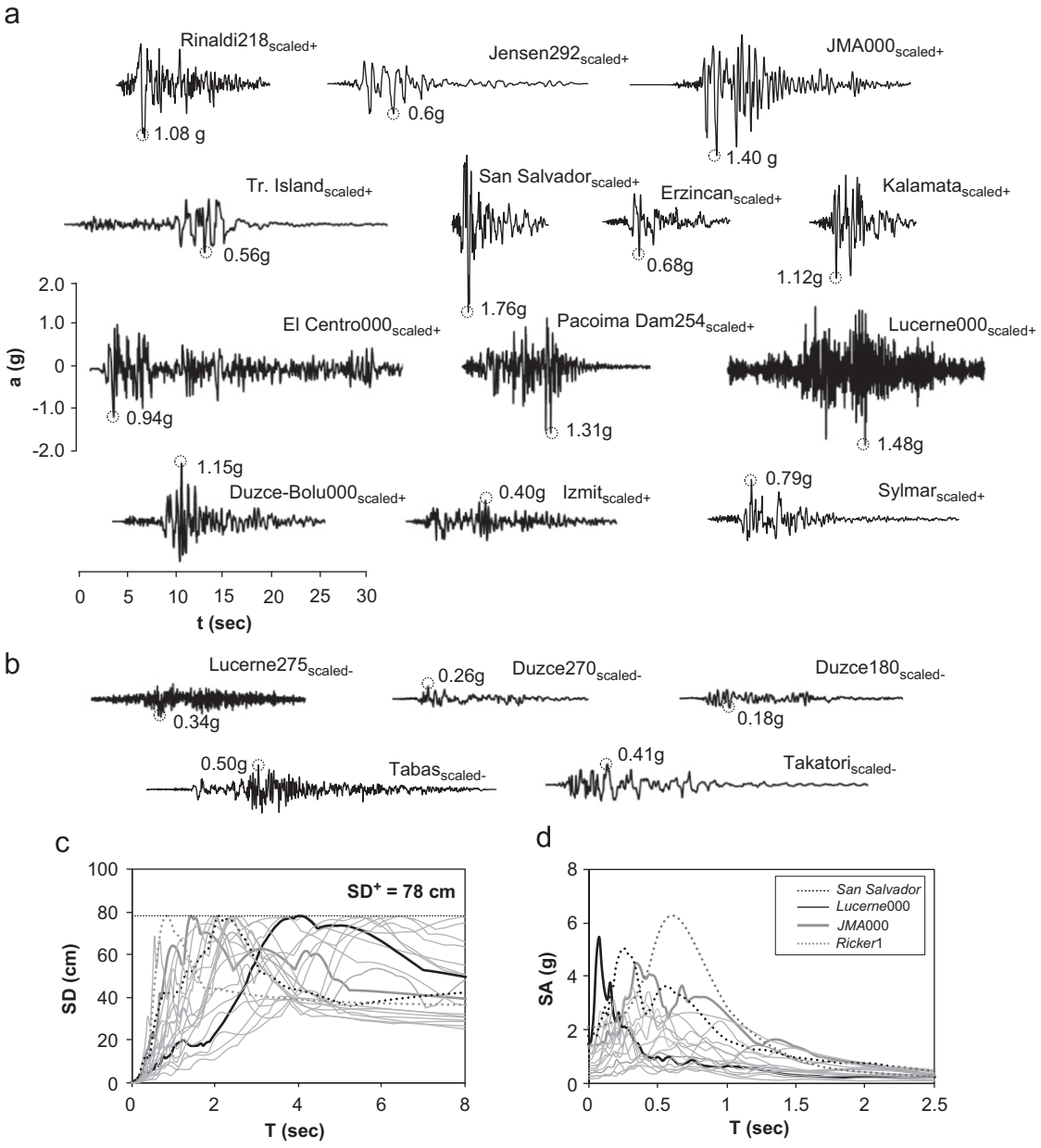

Fig. 13. Real records of devastating earthquakes, used as seismic excitation for the dynamic analysis of the rocking-isolated frame: (a) scaled *up* (in most cases) to achieve SD^+=78 cm, or (b) scaled *down* to achieve SD^+=78 cm; (c) corresponding displacement response spectra, and (d) acceleration response spectra of the scaled seismic motions—four ground motions are distinguished and are further discussed.

8. Insight on ground motion toppling potential

A number of factors affect the toppling potential of a seismic motion while, naturally, *PGA* alone is not an adequate descriptor (e.g. [16,32]). Aiming to better quantify the toppling potential of a ground motion, a destructiveness measure is defined, termed hereafter *cumulative impact pulse velocity*

$$V_{imp,max} = max|V_{imp}| = max\left|\int_0^{t_{tot}} (a - a_{yield})dt\right| \quad (5)$$

where t_{tot} is the total duration of the ground motion and a the acceleration of the seismic motion; a_{yield} is defined as the minimum acceleration that provokes uplifting when applied pseudo-statically, and can be computed as follows:

$$a_{yield} = (SA)_D \frac{M_{ult}^{footing}}{M_{RD}^{C}} \quad (6)$$

where $(SA)_D$ is the design spectral acceleration of the frame, $M_{ult}^{footing}$ the overturning moment capacity of the footing, and M_{RD}^{C} the bending moment capacity of the corresponding column. The role of the aforementioned parameters and the effectiveness of $V_{imp,max}$ is investigated in the sequel for the example problem of the frame founded on $B=1.1$ m footings on nonlinear soil, with $a_{yield}=0.15$ g.

Fig. 14 compares the Lucerne-000 record (Landers, 1992) with the GIC-090 record (San Salvador, 1986), both scaled to $SD^{+}=78$ cm (so that according to the simplified SD_{max} approach, the two records have similar toppling potential). Although the Lucerne record contains a large number of strong motion cycles (peaks) that exceed the yield acceleration a_{yield} (Fig. 14a), it does not contain a large impact velocity pulse $V_{imp,max}$ (Fig. 14b), and is therefore not leading to appreciable foundation rotation (Fig. 14c). In stark contrast, the San Salvador record, despite having significantly smaller number of strong motion cycles (and duration), is characterized by a substantially larger $V_{imp,max}$ (2.04 m/s compared to 0.78 m/s of Lucerne), leading to accumulation of foundation rotation θ and toppling collapse of the structure. The time histories of V_{imp} reveal the key disparity between the two records. A well distinguished pulse produces a pronounced *"impact"* on the structure, forcing it beyond its equilibrium position. Depending on the value of this *velocity impact pulse*, the increase of rotation following this loss of equilibrium may lead to toppling of the structure. This effect is clearly reflected on the time history of footing rotation θ for the San Salvador record: the large *impact velocity pulse* (of 2.04 m/s) at $t=1.4$ s leads to a rather pronounced footing rotation θ of the order of 0.08 rad. Although this rotation is substantially lower than the toppling rotation $\theta_{ult}=0.14$ rad, the deviation from the initial equilibrium position is irrecoverable, with subsequent strong motion cycles generating further accumulation of θ and finally leading to toppling. The Lucerne record is dramatically different. Despite containing a multitude of strong motion cycles with peaks substantially exceeding a_{yield}, none of them has the kinematic characteristics (asymmetry and low frequency, i.e. large duration) to produce large enough V_{imp}. As a result, the produced footing rotation θ fluctuates around zero, while the residual rotation remains relatively small.

The previous comparative example suggests that $V_{imp,max}$ may reveal certain characteristics of a seismic motion, mainly related

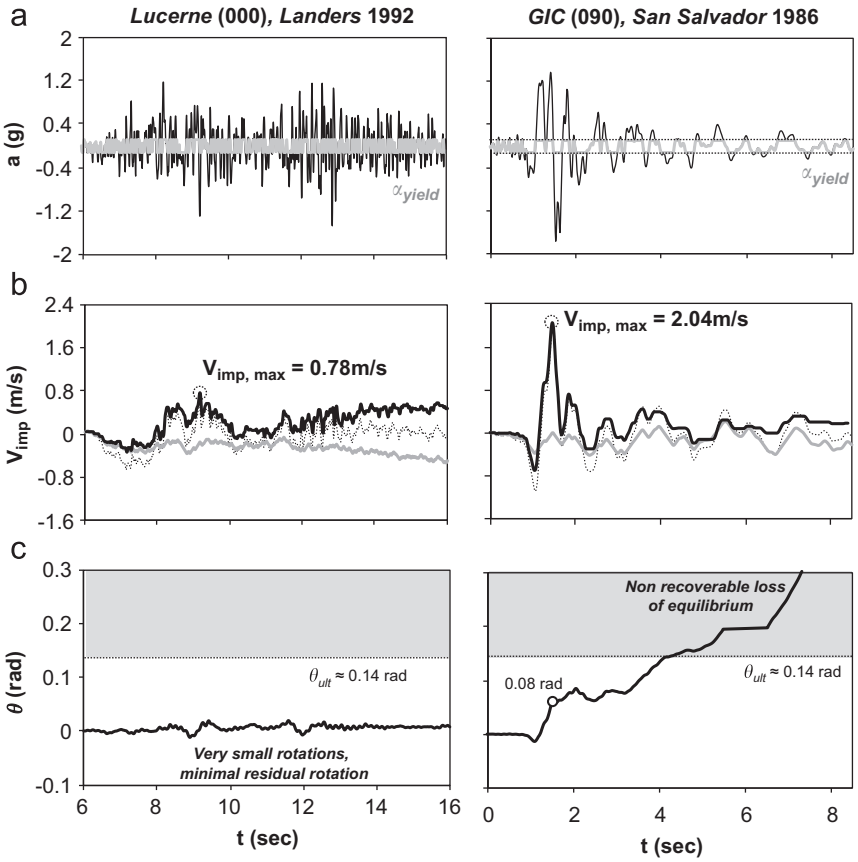

Fig. 14. Nonlinear dynamic time history analysis of the frame (founded on $B=1.1$. m footings) on nonlinear soil—comparison of the effects of the Lucerne-000 (left column) with the GIC-090 (right column) record, both scaled to $SD^{+}=78$ cm: (a) acceleration time histories (the gray lines represent the portion of the acceleration time history, which lies below the critical uplift acceleration α_{yield}); (b) time histories of "*impact velocity*" V_{imp} (bold black line), calculated by subtracting the integral of the acceleration that is lower than α_{yield} (bold gray line) from the integral of the total acceleration (dotted line); and (c) time histories of footing rotation θ.

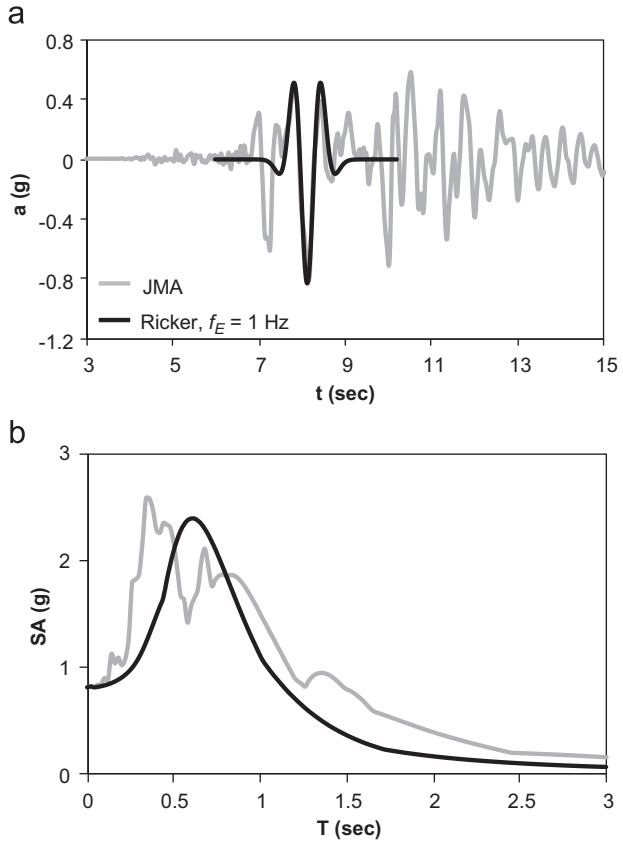

Fig. 15. Comparison of the JMA(000) record with a Ricker 1 (i.e., $f_E=1$ Hz) pulse, scaled to match the PGA of the record: (a) acceleration time histories, and (b) elastic acceleration response spectra *SA*.

to the existence of impact velocity pulses. However, as it will be shown in the sequel through a different example, $V_{imp,max}$ alone is not sufficient to describe the toppling potential of a strong motion. For this purpose, the JMA-000 record (Kobe, 1995) is compared with a Ricker 1 pulse (i.e., $f_E=1$ Hz). As shown in Fig. 15a, the Ricker 1 pulse (scaled with respect to *PGA*) matches quite well with the prevailing strong motion pulse of the JMA record. Quite interestingly, the two motions also match very well in terms of acceleration response spectra (Fig. 15b), despite the obvious differences of their time histories (the JMA record contains a substantial number of strong motion cycles, and much larger duration).

In the context of the simplified SD_{max} approach, the two ground motions are scaled to $SD^+=78$ cm. As shown in Fig. 16a, Ricker 1 needs larger *PGA* (2.2 g) to achieve the same *SD* with the JMA record (1.4 g). Despite "containing" a substantially larger *impact pulse velocity* $V_{imp,max}=2.1$ m/s (Fig. 16b), than the scaled JMA record (of $V_{imp,max}=1.87$ m/s), Ricker 1 is clearly inadequate to provoke toppling collapse of the structure. As shown in Fig. 16c, the first pulse of Ricker 1 generates rotation θ of the order of 0.09 rad, which is recovered, however, during the next (of opposite direction) cycle of motion. Due to the lack of subsequent strong motion pulses, the loss of equilibrium does not culminate with toppling. Dramatically different is the observed system response for the JMA record. While its prevailing strong motion cycle (at $t=8$ s) generates footing rotation θ of similar magnitude to Ricker 1, its subsequent strong motion cycles (which also exceed a_{yield}) produce gradual accumulation of θ, ultimately resulting to toppling collapse of the frame. This implies that the number of strong motion cycles that exceed a_{yield} also plays role in the toppling potential of a seismic motion.

The preceding discussion focused on the safety margins provided by the simplified SD_{max} approach. For this purpose, all seismic motions were scaled to a specific value of SD_{max} ($SD^+=1.1\delta_{ult}$).

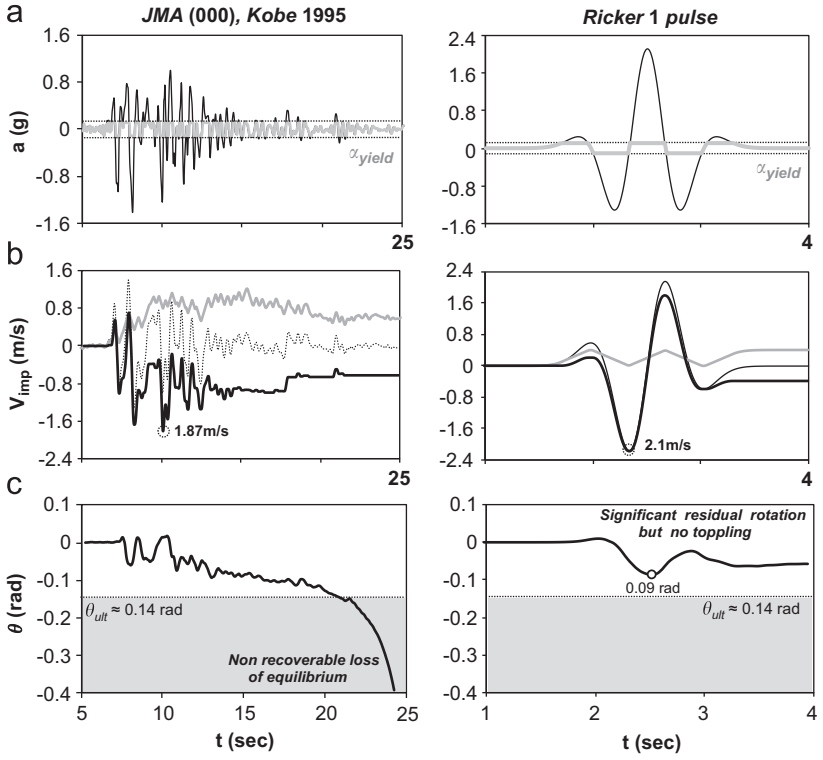

Fig. 16. Nonlinear dynamic time history analysis of the frame (founded on $B=1.1$. m footings) on nonlinear soil—comparison of the effects of the JMA-000 record (left column) with the Ricker 1 pulse (right column), both scaled to $SD^+=78$ cm: (a) acceleration time histories (the gray lines represent the portion of the acceleration time history, which lies below the critical uplift acceleration α_{yield}); (b) time histories of "*impact velocity*" V_{imp} (bold black line), calculated as the time integral of the total acceleration (dotted line) minus the acceleration that is lower than α_{yield} (bold gray line); and (c) time histories of footing rotation θ.

Yet, to achieve SD^+ some of the records had to be un-realistically scaled by factors as high as 7 (Table 1). In reality, however, such *tremendous* seismic motions (e.g. the devastating JMA record scaled-*up* at 1.4 g) have never been recorded and cannot possibly be considered realistic, especially for design purposes. Fig. 17a depicts the original displacement spectra of all ground motions examined, aiming to reveal their real toppling potential. Observe that despite the fact that all ground motions have been recorded during devastating seismic events, in most cases their SD_{max} lies well below the toppling displacement $\delta_{ult}=71$ cm of the $B=1.1$ m footings. In fact, only three records (Takatori-000, Jensen-292, and Tabas) exceed δ_{ult} and had to be scaled-*down*. This observation is of particular importance, since it implies that toppling can be quite *improbable* for real seismic motions, even in case of occurrence of *extremely strong earthquakes* (such as the ones deliberately selected for analysis), and even for *extremely under-designed* footings ($B=1.1$ m).

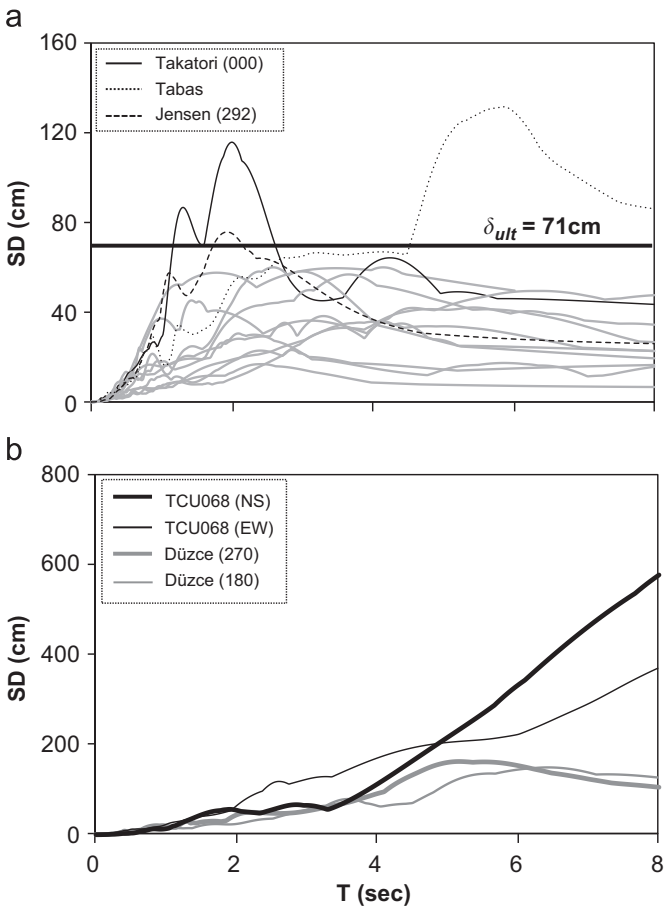

Fig. 17. Displacement response spectra of the *original* records used for the analyses: (a) *"normal"* devastating records, in many cases characterized by forward rupture directivity effects—only in three cases (Takatori-000, Tabas, Jensen-292) $SD_{max} > \delta_{ult}$; (b) *"special cases"* of near-source motions characterized by fling-step effects.

8.1. The paradox of the Chi-Chi record

Although the selected records cover a wide range of seismic motions, none of them is characterized by fling-step effects—a different category of near-source effects, associated with large permanent displacement rather than a large velocity pulse. As shown in the examples of Fig. 17b, such ground motions are characterized by excessively large spectral displacements. For example, the TCU-068 records (Chi–Chi, Taiwan 1999) yield SD_{max} of the order of several meters, i.e. almost an order of magnitude larger than δ_{ult}. With such large SD_{max}, according to the simplified method the structure would easily be lead to toppling collapse. To unravel the response of the system when subjected to this special category of near-source seismic motions, additional analyses are conducted utilizing the original records of Fig. 17b (without scaling). Quite remarkably, even for the *very extreme* case of the TCU-068(NS) record (Fig. 18a), the footing experiences almost negligible rotation θ (Fig. 18b), and the structure is not lead to toppling collapse.

As paradox as this may appear, it is explainable on the basis of the acceleration time history. Despite the large SD_{max}, the yield acceleration a_{yield} is only slightly exceeded, and not for a long duration. This implies that the long-period (almost quasi-static) component of the seismic motion, which is responsible for the excessive SD_{max}, is not really exceeding a_{yield} and, therefore, cannot lead to toppling. As clearly seen in Fig. 18a, the acceleration pulses that do exceed a_{yield} are of much higher frequency, and are not associated with the excessively large SD_{max} of the record. This example reveals the notable conservatism of the simplified approach, for such special cases of near source seismic motions characterized by fling-step effects.

9. Summary and conclusions

In the present study nonlinear FE modeling was employed to study the seismic performance of rocking-isolated frame structures. After investigating the margins of safety of such systems against toppling collapse, a first attempt was made to develop a simplified procedure to estimate the minimum acceptable footing width B_{min}. It was shown that adequate margins of safety against toppling collapse may be achieved, if the toppling displacement

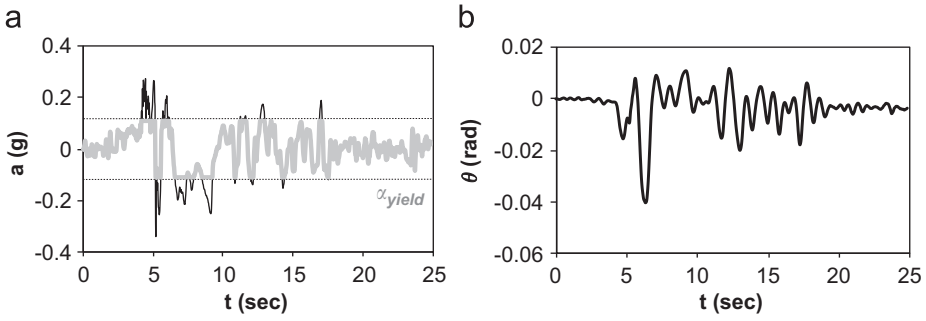

Fig. 18. Nonlinear dynamic time history analysis of the frame subjected to seismic excitation with the TCU-068 (NS) record (Chi–Chi, Taiwan 1999): (a) acceleration time history (the gray-shaded line represents the portion of the acceleration time history, which lies below the yield acceleration α_{yield}—only a very small portion of the record exceeds α_{yield}; (b) time history of footing rotation θ.

capacity of the frame δ_{topl} is sufficiently larger than the seismic displacement *demand* δ_{dem}.

With respect to the *capacity*, the use of an appropriate "equivalent" *rigid-body* is suggested, and shown to yield a conservative estimate of δ_{topl} (which is under-estimated by roughly 30% for the frame structure examined herein). This conservatism stems from the inherent assumptions of the simplified approach, according to which the residual (i.e., for $c > c_{ult}$) bending moment M_{res} of RC members is completely ignored. In this study, M_{res} was reasonably assumed [30] to be of the order of 30% of the corresponding bending moment capacity, which means that the hinged beams will keep contributing a limited amount of restoring moment.

The *demand* is estimated on the basis of the displacement spectrum, and the peak spectral displacement SD_{max} is proposed as a conservative measure of δ_{dem}. The validity and limitations of such approximation were investigated: (a) for a *rigid-block* on *rigid-base*, utilizing rigorous analytical solutions from the bibliography, and (b) for the frame structure on nonlinear soil, by conducting nonlinear dynamic time history analyses. In all cases examined, the simplified SD_{max} approach was shown to yield reasonably conservative estimates of the toppling acceleration a_p. In fact, even for imposed SD_{max} 10% higher than the toppling displacement δ_{ult}, toppling collapse was avoided in most cases (the frame toppled in only 2 out of the 18 seismic excitations). This can be seen as an indication of the degree of conservatism of the simplified SD_{max} approach, for real seismic excitations.

In an attempt to gain further insight on the *toppling potential* of real ground motions, a destructiveness index was defined, termed hereafter *maximum impact pulse velocity* $V_{imp,max}$ (see Eq. (4)). It was shown that the *toppling potential* is a function not only of the imposed *PGA* or SD_{max} , but also of $V_{imp,max}$ and the number of strong motion cycles for which the yield acceleration of the system a_{yield} (see Eq. (5)) is exceeded.

Acknowledgement

The financial support for this paper has been provided under the research project "DARE", which is funded through the European Research Council's (ERC) "IDEAS" Program, in Support of Frontier Research–Advanced Grant, under Contract/number ERC–2–9–AdG228254–DARE.

References

[1] NEHRP. NEHRP recommended provisions for seismic regulations for new buildings and other structures, part 1, provisions, FEMA 368. Washington, DC: Federal Emergency Management Agency; 2000.
[2] Paolucci R, Pecker A. Seismic bearing capacity of shallow strip foundation on dry soils. Soils and Foundations 1997;37(3):95–105.
[3] Pecker A. Capacity design principles for shallow foundations in seismic areas. In: Proceedings of the 11th European Conference on Earthquake Engineering. A.A. Balkema Publishing; 1998.
[4] Pecker A. Aseismic foundation design process, lessons learned from two major projects: the Vasco de Gama and the Rion Antirion bridges. In: Proceedings of the ACI International Conference on Seismic Bridge Design and Retrofit. University of California at San Diego, La Jolla, USA; 2003.
[5] FEMA 356. Prestandard and commentary for the seismic rehabilitation of buildings. 2000.
[6] Gazetas G, Apostolou M, Anastasopoulos I. Seismic uplifting of foundations on soft soil, with examples from Adapazari (Izmit 1999, Earthquake). In: Proceedings of the BGA International Conference on Found Innov, Observations, Design and Practice, Dundee, Scotland; September 25, 2003. p. 37–50.
[7] Psycharis I, Jennings P. Rocking of slender rigid bodies allowed to uplift. Earthquake Engineering and Structural Dynamics 1983;11:57–76.
[8] Yim CS, Chopra AK. Earthquake response of structures with partial uplift on Winkler foundation. Earthquake Engineering and Structural Dynamics 1984; 12:263–81.
[9] Martin GR, Lam IP. Earthquake resistant design of foundations: retrofit of existing foundations. In: Proceedings of the GeoEng 2000 Conference, Melbourne; 2000.
[10] Pecker A, Pender MJ. Earthquake resistant design of foundations: new construction, invited paper. GeoEng 2000;1:313–32.
[11] Faccioli E, Paolucci R, Vivero G. Investigation of seismic soil–footing interaction by large scale cyclic tests and analytical models. In: Proceedings of the 4th International Conference on Recent Advances in Geotechnical Earthquake Engineering and Soil Dynamics, Paper no. SPL-5, San Diego, California; 2001.
[12] Kutter BL, Martin G, Hutchinson TC, Harden C, Gajan S, Phalen JD. Status report on study of modeling of nonlinear cyclic load–deformation behavior of shallow foundations, University of California, Davis, PEER Workshop; March 2003.
[13] Harden C, Hutchinson T. Investigation into the effects of foundation uplift on simplified seismic design procedures. Earthquake Spectra 2006;22(3): 663–92.
[14] Gajan S, Kutter BL. Capacity, settlement, and energy dissipation of shallow footings subjected to rocking. Journal of Geotechnical and Geoenvironmental Engineering, ASCE 2008;134(8):1129–41.
[15] Kawashima K, Nagai T, Sakellaraki D. Rocking seismic isolation of bridges supported by spread foundations. In: Proceedings of the 2nd Japan–Greece Workshop on Seismic Design, Observation, and Retrofit of Foundations, Tokyo, Japan; April 3–4 2007. p. 254–65.
[16] Apostolou M, Gazetas G, Garini E. Seismic response of slender rigid structures with foundation uplifting. Soil Dynamics and Earthquake Engineering 2007; 27(7):642–54.
[17] Paolucci R, Shirato M, Yilmaz MT. Seismic behaviour of shallow foundations: shaking table experiments vs numerical modelling. Earthquake Engineering and Structural Dynamics 2008;37:577–95.
[18] Chatzigogos CT, Pecker A, Salencon J. Macroelement modeling of shallow foundations. Soil Dynamics and Earthquake Engineering 2009;29(6):765–81.
[19] Algie TB, Pender MJ, Orense RP, Wotherspoon LM. Dynamic field testing of shallow foundations subject to rocking. In: Proceedings of the 2009 NZSEE Conference, Christchurch, New Zealand; April 2009.
[20] Pender MJ, Algie TB, Wotherspoon LM, Davies MCR, Toh JCW. Earthquake induced residual displacements of shallow foundations. In: Proceedings of the 2009 NZSEE Conference, Christchurch, New Zealand; April 2009.
[21] Anastasopoulos I, Gazetas G, Loli M, Apostolou M, Gerolymos N. Soil Failure can be used for earthquake protection of structures. Bulletin of Earthquake Engineering 2010;8:309–26.
[22] Gelagoti F, Kourkoulis R, Anastasopoulos I, Gazetas G. Rocking isolation of frames founded on isolated footings. Journal of Earthquake Engineering and Structural Dynamics, accepted for publication.
[23] EC8. Design provisions for earthquake resistance of structures, part 5: foundations, retaining structures and geotechnical aspects, prEN. 1998–5 European Committee for Standardization, Brussels; 2000.
[24] EAK. Greek seismic code, Organization of seismic planning and protection, Athens, Greece; 2000 [in Greek].
[25] Meyerhof GG. Some recent research on the bearing capacity of foundations. Canadian Geotechnical Journal 1963;1(1):6–26.
[26] Vesic AS. Analysis of ultimate loads of shallow foundations. Journal of Soil Mechanics Foundation Division, ASCE 1973;1973(99):45–73.
[27] Anastasopoulos I, Gelagoti F, Kourkoulis R, Gazetas G, in press. Simplified constitutive model for simulation of cyclic response of shallow foundations: validation against laboratory tests. Journal of Geotechnical and Geoenvironmetal Engineering—ASCE, doi:10.1061/(ASCE)GT.1943-5606.0000534.
[28] Gerolymos N, Gazetas G, Tazoh T. Seismic response of yielding pile in nonlinear soil. In: Proceedings of the 1st Greece–Japan Workshop, Seismic Design, Observation, and Retrofit of Foundations, Athens; 2005, 11–12 October. p. 25–36.
[29] Imbsen & Associates, Inc. XTRACT—cross section analysis program for structural engineer, Ver. 3.0.3, California; 2004.
[30] Vintzileou E, Tassios TP, Chronopoulos M. Experimental validation of seismic code provisions for RC columns. Engineering Structures 2007;29:1153–64.
[31] Bielak J. Base moment for a class of linear Systems. Journal of the Engineering Mechanics Division 1969;95.
[32] Makris N, Roussos Y. Rocking response of rigid blocks under near source ground motions. Géotechnique 2000;50(3):243–62.
[33] Priestley MJN, Evison RJ, Carr AJ. Seismic response of structures free to rock on their foundations. Bulletin of the New Zealand National Society for Earthquake Engineering 1978;11(3):141–50.
[34] Makris N, Konstantinidis D. The rocking spectrum and the limitations of practical design methodologies. Earthquake Engineering and Structural Dynamics 2003;32(2):265–89.
[35] Housner GW. The behavior of inverted pendulum structures during earthquakes. Bulletin of the Seismological Society of America 1963;53(2):404–17.
[36] Ishiyama Y. Review and discussion on overturning of bodies by earthquake motions. Building Research Institute, Research paper 85, Ministry of Construction, Japan; 1980.
[37] Koh AS, Spanos P, Roesset JM. Harmonic rocking of rigid block on flexible foundation. Journal of Engineering Mechanics, ASCE 1986;112(11):1165–80.
[38] Gerolymos N, Apostolou M, Gazetas G. Neural network analysis of overturning response under near-fault type excitation. Earthquake Engineering and Engineering Vibration 2005;4(2):213–28.
[39] Zhang J, Makris N. Rocking response of free-standing blocks under cycloidal pulses. Journal of Engineering Mechanics, ASCE 2001;127(5):473–83.